Fabiato, A. (1985) *Basic Res. Cardiol. 80 (Suppl. 2)*, 83–87.
Fabiato, A., & Fabiato, F. (1975) *J. Physiol. (London) 249*, 469–495.
Fiskum, G., & Lehninger, A. L. (1982) in *Calcium and Cell Function* (Cheung, W. Y., Ed.) Vol. II, pp 39–80, Academic, New York.
Fleckenstein, A. (1981) in *New Perspectives in Calcium Antagonists* (Weiss, G. B., Ed.) pp 59–81, American Physiological Society, Bethesda, MD.
Fleischer, B., & Smigel, M. (1978) *J. Biol. Chem. 253*, 1632–1638.
Garlick, P. B., Radda, G. K., & Seeley, P. J. (1979) *Biochem. J. 184*, 547–554.
Hirasawa, K., & Nishizuka, Y. (1985) *Annu. Rev. Pharmacol. Toxicol. 25*, 147–170.
Hirche, H. J., Franz, C. H. R., Bos, L., Bissig, R., Lang, R., & Schramm, M. (1980) *J. Mol. Cell. Cardiol. 12*, 579–593.
Hokin, E. L. (1985) *Annu. Rev. Biochem. 54*, 205–235.
Imai, A., & Gershengorn, M. C. (1987) *Nature (London) 325*, 726–728.
Jergil, B., & Sundler, R. (1983) *J. Biol. Chem. 258*, 7968–7973.
Jones, L. R., & Besch, H. R., Jr. (1984) *Methods Pharmacol. 5*, 1–12.
Jones, L. R., Besch, H. R., Jr., Fleming, J. W., McConnaughey, M. M., & Watanabe, M. M. (1979) *J. Biol. Chem. 254*, 530–539.
Kirchberger, M. A., & Antonetz, T. (1982) *J. Biol. Chem. 257*, 5685–5691.
Kirchberger, M. A., Tada, M., & Katz, A. M. (1974) *J. Biol. Chem. 249*, 6166–6173.
Kirchberger, M. A., Borchman, D., & Kasinathan, C. (1986) *Biochemistry 25*, 5484–5492.
Mattern, J., Satumtira, N., & Quist, E. (1985) *Pharmacologist 27*, 170.
Moore, J. P., Smith, G. A., Hesketh, T. R., & Metcalfe, J. C. (1983) *Biochem. J. 212*, 691–697.
Ochs, R. (1986) *Trends Biochem. Sci. (Pers. Ed.) 11*, 388–389.
Parries, G. S., & Hokin-Neaverson, M., (1984) *Biochemistry 23*, 4785–4791.
Schacht, J. (1978) *J. Lipid Res. 19*, 1063–1067.
Smith, P. D., Liesegang, G. W., Berger, R. L., Czerlinski, G., & Podolsky, R. J. (1984) *Anal. Biochem. 143*, 188–195.
Suzuki, T., & Wang, J. H. (1987) *J. Biol. Chem. 262*, 3880–3885.
Tada, M., Kirchberger, M. A., & Katz, A. M. (1975) *J. Biol. Chem. 249*, 6166–6173.
Takenawa, T., & Egawa, K. (1977) *J. Biol. Chem. 252*, 5419–5423.
Tomlins, B., Harding, S. E., Kirby, S. K., Polle-Wilson, P. A., & Williams, A. J. (1986) *Biochim. Biophys. Acta 856*, 137–143.

Composition of Octyl Glucoside–Phosphatidylcholine Mixed Micelles

Ofer Eidelman,*,†,§ Robert Blumenthal,‡ and Anne Walter†,‖

Section on Membrane Structure and Function, LMMB, National Cancer Institute, National Institutes of Health, Building 10, Room 4B56, Bethesda, Maryland 20892, and Department of Physiology and Biophysics, Wright State University School of Medicine, Dayton, Ohio 45435

Received August 11, 1987; Revised Manuscript Received December 10, 1987

ABSTRACT: The compositon of mixed micelles of egg phosphatidylcholine (PC) and octyl glucoside was studied by a novel technique based on measuring resonance energy-transfer efficiency between two fluorescent lipid probes present in trace amounts. Equations were derived for calculating the stoichiometry of the composition of mixed micelles from the energy-transfer measurements. These were applied to determining the average number of lipid molecules in the octyl glucoside–egg PC mixed micelle as a function of detergent concentration. The average number of detergent molecules in these mixed micelles also was determined by varying the lipid concentration. The stoichiometry of egg PC–octyl glucoside mixed micelles was independent of lipid concentration in the range studied (0–500 μM). The dependence of mixed micelle stoichiometry on the concentration of aqueous (monomeric) octyl glucoside is consistent with the assumptions of ideal mixing of the two amphiphiles in the mixed micelles and that mixed micelles can be treated as a distinct phase.

Solubilization of biological membranes by detergents and formation of a bilayer membrane from a mixture of lipids and membrane proteins dissolved in detergent are two important steps in achieving functional reconstitution of membrane proteins. Knowledge of the behavior of the lipid–detergent–protein system, and its dependence on various conditions (concentrations of detergent, temperature, ionic strength, etc.), is of importance to optimize solubilization and functional insertion of the membrane proteins into the lipid bilayer. For these reasons, we have been studying the physicochemical details of a lipid–detergent mixture, egg phosphatidylcholine (PC)[1]–octyl glucoside. Characterization of this system, in the

‡National Institutes of Health.
§Present address: Department of Biological Chemistry, The Hebrew University of Jerusalem, Givat-Ram, Jerusalem 91904, Israel.
‖Wright State University School of Medicine.

[1] Abbreviations: RET, resonance energy transfer; HEPES, *N*-(2-hydroxyethyl)piperazine-*N*′-2-ethanesulfonic acid; NBD-PE, *N*-(7-nitro-2,1,3-benzoxadiazol-4-yl)phosphatidylethanolamine; PC, phosphatidylcholine; Rho-PE, *N*-(lissamine rhodamine B sulfonyl)phosphatidylethanolamine; SUV, small unilamellar vesicle(s); OG, *n*-octyl β-D-glucopyranoside; EDTA, ethylenediaminetetraacetic acid; cmc, critical micelle concentration; $C_{12}E_8$, *n*-dodecyl octaethylene glycol monoether.

absence of protein, can serve as a "bench-mark" against which data from protein–lipid–detergent mixtures may be compared.

The egg PC–OG phase diagram (Jackson et al., 1982; Ollivon et al., 1988) shows two reversible major transitions occurring during both addition of OG to liposome suspensions and removal of OG from micellar suspension. These transitions divide the phase diagram into three parts: a lamellar domain at low detergent concentrations, a micellar domain at high detergent concentrations, and a mixed phase (lamellar and micellar) domain between them. The present study concentrates on the molecular composition of the structures that are found in the micellar domain. We have developed a technique for determining the average number of lipid molecules in a mixed micelle based on measuring resonance energy transfer (RET) between two lipid probes, NBD-PE and Rho-PE, present at trace concentrations with unlabeled PC. These measurements are used to determine the composition of lipid–detergent mixed micelles.

The structure and composition of detergent micelles and detergent–lipid mixed micelles have been studied by several methods such as light scattering, electron microscopy, surface tension, X-ray and neutron diffraction, and gel chromatography [e.g., see Dennis (1986); Schurtenberger et al. (1985); Fromherz and Ruppel (1985); and Clint (1975)]. These techniques measure physical properties of the micelles and deduce the composition of the micelles. The method described here is aimed at measuring directly the number of lipid molecules in the mixed micelle. By varying the lipid concentration, we could also determine the detergent content of the mixed micelles, and the physical dimensions of these mixed micelles were estimated from the determined composition. The next section outlines the theoretical basis of the method, the justification of the assumptions, and the limitations of the method. The approach was then implemented to describe the OG–PC mixed micelles.

Theory

This method for determining the composition of mixed micelles is based on the properties of resonance energy transfer between fluorescent lipid probes and on the probability of finding both donor and acceptor probe molecules in the same mixed micelle. The presence of an acceptor molecule in a micelle will cause maximal fluorescence quenching of donor molecules in that micelle, provided the mixed micelles have a diameter on the order of, or smaller than, the characteristic energy-transfer distance (R_0). Using the theory of Fung and Stryer (1978) and the data of Struck et al. (1981), we estimate R_0 for the pair NBD-PE and Rho-PE to be 5–8 nm. Thus, the degree of donor (NBD-PE) fluorescence quenching by energy transfer to the acceptor (Rho-PE) is related to the chance of having a mixed micelle containing both NBD-PE and Rho-PE. This chance depends on the average number of lipid molecules per mixed micelle (n_{PC}) and on the mole fraction of Rho-PE in the lipid mixture. The calculations of this chance are given below. Experimentally measured values of NBD fluorescence quenching were used, in conjuction with these calculations, to determine the average number of lipid molecules per mixed micelle as a function of [OG].

The assumptions on which the analysis is based are the following. (1) The distribution of lipid molecules among the mixed micelles is independent of their identity. This means that the distribution of lipids in the mixed micelles depends primarily on interactions of the hydrophobic tails of the molecules rather than the hydrophilic head groups, so that the fluorescent probes NBD-PE and Rho-PE are indistinguishable from PC molecules. (2) One Rho-PE molecule in a mixed micelle is sufficient for complete quenching of the fluorescence of NBD moieties in the same micelle. This assumption is based on the fact that the maximal distance between two head groups in a spherical micelle is the diameter of the micelle which must be smaller than twice the extended length of the amphiphiles, i.e., less then 5 nm. This is smaller than the average distance between NBD-PE and Rho-PE in a membrane containing 0.8 mol % Rho-PE (~8 nm), in which condition it has been shown [e.g., see Struck et al. (1981)] that maximal quenching of NBD fluorescence occurs. As shown below, the average distance between probes in the largest mixed micelles, for which the assumptions have been found to be valid, is about 6 nm (see Discussion and Table I). (3) The lipid–detergent mixed micelles have a unimodal distribution (i.e., with a single peak), and the number of lipid molecules per mixed micelle follows a Poisson distribution. The need for the latter part is not strict, since two other very different distributions, namely, a δ function and a square one, gave results similar to eq 4, but the derivation resulted in a relatively simpler equation with this assumption. The validity of the assumption about unimodal distribution of the OG–PC mixed micelles had been shown by gel filtration chromatography (Ollivon et al., 1988; M. Ollivon and A. Walter, unpublished results). Unimodal distribution was also indicated from the results of quasi-elastic light-scattering measurements (see below). The relation between NBD fluorescence quenching and the average number of lipid molecules per mixed micelle, based on the above assumptions, is calculated below by using the Poisson distribution function:

$$P(n,\lambda) = \frac{1}{n!}\lambda^n \exp(-\lambda) \quad (1)$$

where $P(n,\lambda)$ is the probability of finding a mixed micelle containing exactly n lipid molecules when the average number of lipid molecules per micelle (n_{PC}) is λ. The same distribution can be invoked for the probability of finding a mixed micelle containing exactly n Rho-PE molecules, with an average per micelle of $\lambda = n_{PC}\rho$, where ρ is the mole fraction of Rho-PE. Thus, the fraction of mixed micelles containing no Rho-PE molecues (i.e., $n = 0$) is

$$P(0,n_{PC}\rho) = \exp(-n_{PC}\rho) \quad (2)$$

Since we assume that the distribution of NBD-PE is independent of Rho-PE, $P(0,n_{PC}\rho)$ is also the probability of finding an NBD-PE molecule in a micelle without Rho-PE. Thus, the fraction of unquenched NBD fluorescence (f_u) is equal to $P(0,n_{PC}\rho)$:

$$f_u = \exp(-n_{PC}\rho) \quad (3)$$

or

$$n_{PC} = -\frac{1}{\rho}\ln f_u \quad (4)$$

The above equation was also obtained from a rigorous (and tedious) derivation using the assumptions of a Poisson distribution of n_{PC} and binomial distribution of the three kinds of lipid molecules.

Materials and Methods

Materials. NBD-PE, Rho-PE, and egg PC were from Avanti Polar Lipids (Birmingham, AL); octyl glucopyranoside was from Calbiochem (Irvine, CA). The buffer solution used was 100 mM NaCl, 10 mM HEPES, 0.1 mM EDTA, and 0.02% sodium azide, pH 7.4.

Preparation of Lipid Vesicles. Egg PC (10 mg/mL in chloroform) was mixed with NBD-PE (0.8 mol %) or with

both NBD-PE and Rho-PE (0.8 mol % or as indicated). The lipid was dried as a film under a stream of nitrogen and held for at least 1 h under vacuum. Vesicles were then formed by hydrating the lipid with the buffer solution and probe sonication (Heat Systems–Ultrasonics Model W-375) until the suspension cleared. Final lipid concentration was measured by total phosphate (Ames & Durbin, 1960). Fluorescent probe concentrations were determined by absorbance measurements in ethanol (NBD, ϵ_{465} = 28 100 M^{-1} cm^{-1}; rhodamine, ϵ_{573} = 114 000 M^{-1} cm^{-1}).

Fluorescence Measurements. A suspension of the required amount of vesicles labeled with NBD-PE alone or with both NBD-PE and Rho-PE in buffer solution was placed in a fluorometer cuvette and was stirred by a magnetic bar on the bottom and a motor-driven Teflon paddle (Spectrocell, Oreland, PA) from the top. Fluorescence was measured with an SLM-8000 fluorometer (SLM Instruments, Urbana, IL) equipped with a thermostatted cuvette holder set at 25 °C. Excitation was at 473 nm and emission at 535 nm with both slits set at 8 nm. Continuous addition of octyl glucoside to the cuvette was done as previously described (Ollivon et al., 1988), by pumping stock solution of octyl glucoside (100–400 mM in buffer solution) via polyethylene tubing connected to a Hamilton syringe mounted on a syringe pump, at a rate of about 11 μL/min (usually ~2 mM/min rate of change in [octyl glucoside]). Fluorescence intensity data were collected in the ratio mode, at 2- or 10-s intervals.

Light-scattering measurements were performed by using a BI-2030-AT digital correlator (Brookhaven Instrument Co., Holtsville, NY) with Model 95 argon ion laser (Lexel Co., Palo Alto, CA) excitation.

Data Analysis. Fluorescence intensity data were collected for pairs of samples, with identical lipid and NBD-PE concentrations; one also was labeled with Rho-PE. Fluorescence intensity values of the samples labeled with both NBD-PE and Rho-PE were divided by the values corresponding to the same time point of the NBD-only sample to get f_u, the fraction of NBD fluorescence not quenched by rhodamine. This procedure corrected for both sample dilution and the observed effect of OG on NBD fluorescence. The f_u values were used to calculate the averge number of lipid molecules per mixed micelle (n_{PC}) according to eq 4. The concentration of OG for each data point was calculated from the time and the known rate of OG addition. Smoothing of the calculated n_{PC} values was done by moving-window-averaging of 10 values (the change in [OG] in the window was less than 0.5 mM), and then the average (±SD) of [OG] was determined for all the data points with n_{PC} between n and $n + 1$.

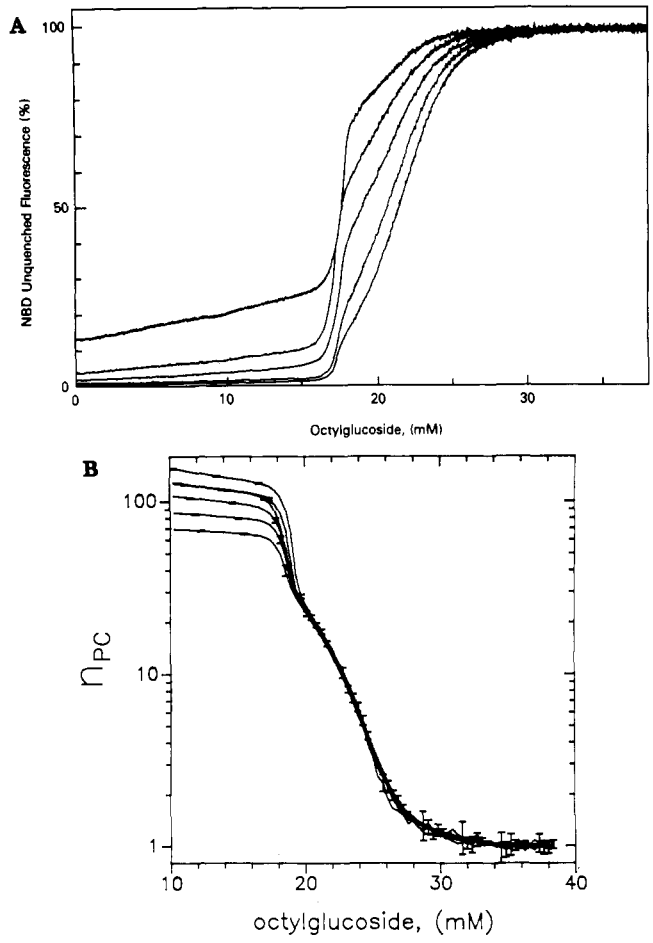

FIGURE 1: Effect of octyl glucoside concentration on NBD-PE fluorescence quenching by Rho-PE, and the average number of lipid molecules per mixed micelle calculated from these data. (A) Egg PC SUV were prepared with 0.8 mol % NBD-PE and several concentrations of Rho-PE (from top to bottom, 0.7, 1.5, 2.1, 3.5, or 5 mol %). The SUV were suspended at 25 μM total lipid in a fluorometer cuvette at 25 °C.. NBD fluorescence intensity was measured as the lipids were progressively dissolved by slow addition of OG. The percentage of unquenched NBD fluorescence was calculated by dividing the observed fluorescence intensity at any given [OG] by the fluorescence intensity at the same [OG] of an equivalent sample labeled only with NBD-PE. (B) The average numbers of lipid molecules per mixed micelle (n_{PC}) were calculated according to eq 4 from the data in (A). The lines are in the same order of Rho-PE concentrations as in (A). The data were smoothed by averaging groups of 10 points in each curve (about 0.5 mM change in [OG]), and the error bars denote the standard deviations of the values in each group (only a few are shown). The data are presented on a logarithmic scale to clarify the details both at high and at low n_{PC}.

RESULTS

Determination of n_{PC} as a Function of [OG]. The validity of the assumptions, on which the calculations of the average number of lipid molecules per mixed micelle are based (eq. 4), was assessed by calculating n_{PC} as a function of [OG] at several values of Rho-PE mole fraction (ρ). The actual value of f_u for any given micelle size is expected to depend on ρ, but if the assumptions are valid, the calculated values of n_{PC} should only depend on [OG] and [PC] and not on ρ. The following experiment was designed to check this: five samples of PC SUV were prepared with the same concentration of total lipid (25 μM) and of NBD-PE (0.8 mol %) but containing different amounts of Rho-PE (0.7, 1.5, 2, 3.5, and 5 mol %, respectively). NBD fluorescence was measured during dissolution by octyl glucoside, and the fraction of unquenched NBD-PE fluorescence (Figure 1A) was calculated as described under Materials and Methods. The values of the average number of PC molecules per mixed micelle (n_{PC}) for each sample, calculated according to eq 4, are shown in Figure 1B as a function of [OG]. At concentrations of OG where the OG–PC system is expected to have lamellar structures (Ollivon et al., 1988), the curves for the different Rho-PE contents diverge, as expected, since the assumption that the structures are small enough that a single Rho-PE is sufficient to quench any NBD-PE in that structure is clearly not valid in the lamellar phase.

However, for [OG] > 18 mM, where only the micellar phase is found at this [PC] (Ollivon et al., 1988), the five different curves converge. Statistical analysis of the significance of this convergence was done by comparing the differences between 10 point averages of values on each curve with their standard deviations (see Materials and Methods). Above 18 mM (i.e., for n_{PC} < 30), the differences between the various average values at any [OG] were found to be less than the corre-

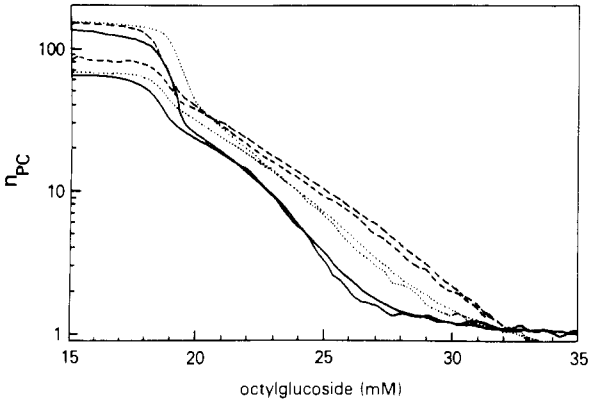

FIGURE 2: Effect of egg PC concentration on the average number of lipid molecules per mixed micelle. The values of n_{PC} as a function of [OG] were determined as in Figure 1 for egg PC SUV at three different lipid concentrations: 25 mM (solid lines), 100 mM (dotted lines), and 250 mM (dashed lines). The SUV were labeled with either 0.7 or 5 mol % Rho-PE and 0.8 mol % NBD-PE. At high [OG], the calculated n_{PC} appears to be a function of [PC] and not of Rho-PE mole percent, while at low [OG] we observe the converse, as predicted.

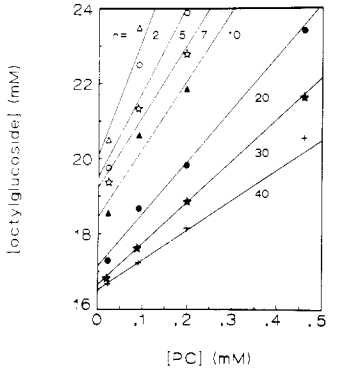

FIGURE 3: Total concentration of OG needed to attain a given n_{PC} is a linear function of the concentration of egg PC. The values of n_{PC} were determined, as a function of [OG], for egg PC labeled with NBD-PE and Rho-PE. The concentration of OG at which mixed micelles of a given n_{PC} were observed was estimated from the average [OG] of all the data points for which the integer part of the calculated n_{PC} was equal to the value indicated. The solid lines are the linear regression fits to the data for each n_{PC}.

sponding standard deviations (Figure 1B). The opposite was true below 18 mM (n_{PC} above 30), where the differences between the various curves were much larger than the standard deviations.

Determining n_{PC} at Different Concentrations of PC. The experiments described above were repeated at three different concentrations of PC (25, 100, and 250 μM total lipid) and two mole fractions of Rho-PE (0.7% and 5%). The results, given in Figure 2, showed that for $n_{PC} < 30$ the curves converged according to [PC] while above that value they converged according to the Rho-PE mole fraction. This shows that the assumptions used in deriving eq 4 hold for structures occurring in the range of [PC] employed, for $[OG]_{aq} > 18$ mM. Second, as [PC] increases, higher [OG] is required in order to obtain any given value of n_{PC}. This observation suggests that the calculated value of n_{PC} represents a feature of lipid–detergent structures for which the OG/PC ratio is determined by n_{PC}. To check this hypothesis, we looked at a wider range of [PC] and analyzed the data as depicted in Figure 3.

The relation between n_{PC} and the concentrations of OG and of egg PC was studied by determining n_{PC} as a function of $[OG]_{total}$ at four different concentrations of PC. Figure 3 shows the dependence on [PC] of the average value of $[OG]_{total}$

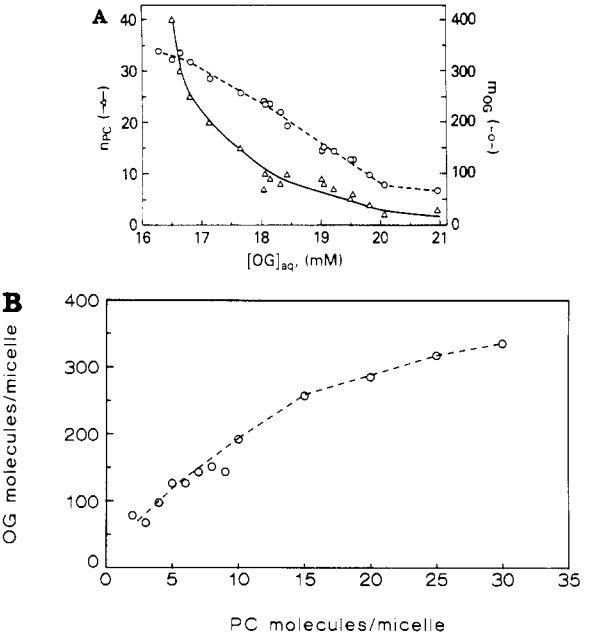

FIGURE 4: Stoichiometry of egg PC–octyl glucoside mixed micelles. The data of the experiment described in Figure 3 were used to determine the values of n_{PC}, of m_{OG} (the average number of octyl glucoside molecules per mixed micelle), and of $[OG]_{aq}$ (the concentration of aqueous OG accompanying mixed micelles of each given composition). n_{PC} was derived from the original data according to eq 4, and m_{OG} was derived according to eq 5 from the slopes of the regression lines of Figure 3, and $[OG]_{aq}$ from the intercepts of these regression lines. (A) m_{OG} and n_{PC} as a function of $[OG]_{aq}$. (B) The relationship between m_{OG} and n_{PC}.

for all data points for which n_{PC} is between the indicated n and $n + 1$. We included the $n = 40$ line, although the assumptions might not be valid there (see Figure 1B). The lines are the least-squares linear regression of the corresponding data points. The linearity of these dependencies is explained by recalling that the total amount of octyl glucoside in the cuvette is divided into two categories, one which is associated with lipid–detergent structures and another ($[OG]_{aq}$) which is not associated with lipid (i.e., in monomeric form). If the nature of the lipid–detergent associations in the mixed micellar domain depends on both [OG] and [PC] (as, for instance, in bimolecular aggregation), then the dependencies in Figure 3 should not be linear but curved. On the other hand, if mixed micellar structures of a given composition are in equilibrium with a certain concentration of monomeric OG (i.e., their composition is determined by the activity of $[OG]_{aq}$), then the total concentration of octyl glucoside ($[OG]_{total}$) at which a given structure comprised of n PC molecules and m OG molecules is found should be a linear function of the amount of lipid [see, e.g., Ollivon et al. (1988)]:

$$[OG]_{total} = [OG]_{aq} + \frac{m_{OG}}{n_{PC}}[PC] \qquad (5)$$

Thus, the slopes of the linear regression lines give the mole ratio betwen octyl glucoside and PC in mixed micelles of the respective values of n_{PC}, while the intercepts estimate the free concentration of octyl glucoside in equilibrium with each composition.

Octyl Glucoside and PC Stoichiometry in Mixed Micelles. The regression lines of Figure 3 were used to calculate the average number of octyl glucoside molecules per mixed micelle (m_{OG}) according to eq 5. The values of n_{PC} and m_{OG} are presented as a function of $[OG]_{aq}$ in Figure 4A, and against each other in Figure 4B. Figure 4A shows that when $[OG]_{aq}$ increased, both n_{PC} and m_{OG} decreased, and Figure 4B that

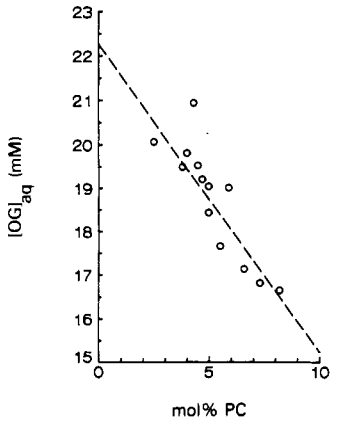

FIGURE 5: Relationship between $[OG]_{aq}$ and mixed micellar composition. The aqueous concentrations of OG in equilibrium with mixed micelles of a given composition (i.e., the intercepts of the regression lines in Figure 3) were plotted against the mole fraction of PC in the mixed micelles. The straight line is the least-squares linear regression of the points.

the ratio of m_{OG} to n_{PC} decreased with increasing n_{PC}. These two observations, combined, described a progressive change in the composition of mixed micelles as egg PC was dissolved by OG from above the transition to the mixed micellar phase (Ollivon et al., 1988) until the lipid molecules were completely dispersed in different micelles. Near the transition from lamellar structures to pure mixed micelles, the structures were large, containing more than 30 PC molecules and more than 400 OG molecules. As [OG] increased, the mixed micelles became smaller as both n_{PC} and m_{OG} decreased, while the mole fraction of PC in them decreased.

Mixed Micelles Are in Equilibrium with Aqueous Octyl Glucoside. The data presented above show that mixed micelles occur at OG concentrations below the critical micellar concentration (20.5 mM; Ollivon et al., 1988). This is expected and well described for solutions of mixed amphiphiles [e.g., see Tanford (1980), Clint (1975), and Ollivon et al. (1988)]. The data of Figure 3 were used to study the effect of $[OG]_{aq}$ on the composition of the mixed micelles. Figure 5 shows that $[OG]_{aq}$ depends in a linear fashion on the mole fraction of PC in the micelle [$\chi_{PC} = n_{PC}/(m_{OG} + n_{PC})$]. Least-squares linear regression of the data extrapolates to an intercept of 22.3 mM at $\chi_{PC} = 0$, in good agreement with the measured value of the critical micellar concentration of OG [25 mM (Shinoda et al., 1961); 22 mM (Jackson et al., 1982); 20.5 mM (Ollivon et al., 1988)].

Discussion

The objectives of the present work were first to develop a new method for studying the composition of mixed micelles and then to use this method for studies of the mixed micellar domain of aqueous mixtures of PC and OG. The method relies on measuring resonance energy-transfer (RET) quenching between two lipid probes. RET is used extensively as a "spectroscopic ruler" for determining distances or surface densities of probes (Fung & Stryer, 1978). However, in the present method, it is used in a different manner to determine the probability of having a micelle containing a donor, but not an acceptor, probe. This different application of RET is feasible because the particles studied are small structures for which quenching is all-or-none depending on the presence of donor and acceptor lipid probes in the same micelle. The degree of donor fluorescence quenching gives a direct measure of this probability, which is related to the average number of lipid molecules in the mixed micelle, and to the mole fraction of acceptor lipids (see eq 4 under Theory), provided the following three requirements are met: (a) that the distribution of probes among micelles is indistinguishable from that of the predominant lipid: (b) that a single Rho-PE in a micelle is enough to quench the fluorescence of NBD-PE in that micelle; (c) that the distribution of mixed micelle size is unimodal.

Assessing the Validity of the Assumptions. The experiment shown in figure 1 was designed to address the question of the validity of the assumptions. First, if there were a preferential segregation of labeled molecules into probe-rich micelles, then complete NBD fluorescence quenching should be observed near the lamellar to micellar transition (where large mixed micelles containing both NBD-PE and Rho-PE are expected to be found), changing abruptly to no quenching when the average number of probe molecules per mixed micelle became about 1 (so that micelles with only NBD-PE could be found). On the other hand, if the presence of a single Rho-PE were not enough to fully quench the fluorescence of all NBD moieties in the same micelle, then samples with higher Rho-PE content should have given a higher calculated value of n_{PC} than those with lower Rho-PE content, as there would have been higher chance of having more than one Rho-PE molecule per micelle. However, as clearly shown in figure 1B, the calculated n_{PC} values coincide for all samples spanning a 7-fold range of Rho-PE content for $n_{PC} < 30$, consistent with unbiased distribution of probe molecules and with complete quenching by a single Rho-PE. There does seem to be a region of the PC–OG phase diagram where the latter assumption might not hold, specifically (for this range of [PC]) the range of [OG] between ~16.8 mM, where the transition to pure micellar phase occurs (Ollivon et al., 1988), and 18 mM, where n_{PC} becomes smaller than 30 (Figure 1). This interpretation of the results means that for $n_{PC} > 30$, the diameter of the mixed micelles becomes so large that a single Rho-PE molecule cannot fully quench the fluorescence of all NBD-PE probes in that micelle. The results of Figure 1B and Figure 2 show that the amount of NBD fluorescence quenching (and thus of the calculated values of n_{PC}) depends on the mole fraction of Rho-PE as predicted by eq 4, thus supporting the validity of the assumptions on which the derivation of this equation is based.

The validity of the third assumption, regarding the unimodality of the OG–PC mixed micelles size distribution, had been shown before (Ollivon et al., 1988; M. Ollivon and A. Walter, unpublished observations) using gel exclusion chromatography. We have attempted to corroborate these observations with additional quasi-elastic light-scattering determinations. Unfortunately, the size of the micelles, which were prepared to be on the $n_{PC} = 10$ line (Figure 3) and estimated to be about 4 nm (Table I), was found to be below the resolution limit of the apparatus used (ca. 10 nm). Nevertheless, these measurements could show that in this case there could not have been a substantial population of micelles with sizes $\gtrsim$10 nm, that would have been expected to occur in a bimodal distribution with an average size of 4 nm. Thus, the technique presented in this work is complementary to quasi-elastic light scattering in two aspects: size range and lipid concentration. Whereas light scattering is useful for determining the size of micelles larger than ~10 nm (for the readily available instruments) and at relatively high lipid concentrations, the present technique is useful for micelles smaller than 5 nm (i.e., in which a single acceptor molecule per micelle can quench a donor molecule at any position in the micelle), and it is sensitive enough to measure at very low micelle concentrations (down to 20 μM lipid which is equivalent to a micelle number concentration of $\sim 6 \times 10^{14}$/mL).

Table I: Volumes and Surface Areas of Mixed Micelles: Comparison of Mixed Micelle Surface Area with That of Ellipsoids Having the Same Volume and a Minor Axis of 1.16 nm[a]

		surface area (nm^2)			ellipsoid major axis (nm)	
			ellipsoid			
n_{PC}	volume of micelle[b] (nm^3)	micelle[c]	oblate[d]	prolate[d]	oblate	prolate
2–3	22 ± 9	32 ± 14	40 ± 13	46 ± 19	2.1 ± 0.5	3.8 ± 1.6
5–6	41 ± 9	60 ± 14	68 ± 13	84 ± 18	2.9 ± 0.3	7.3 ± 1.6
7–8	72 ± 12	107 ± 19	110 ± 16	148 ± 25	3.9 ± 0.3	12.8 ± 2.1
10–11	76 ± 11	110 ± 17	115 ± 15	155 ± 23	4.0 ± 0.3	13.5 ± 2.0
15–16	74 ± 6	104 ± 9	113 ± 8	152 ± 13	3.9 ± 0.2	13.2 ± 1.1
20–21	93 ± 12	130 ± 19	138 ± 16	190 ± 25	4.4 ± 0.3	16.6 ± 2.2
25–26	98 ± 8	133 ± 13	144 ± 11	199 ± 17	4.5 ± 0.6	17.3 ± 1.5
30–31	109 ± 9	147 ± 14	160 ± 13	222 ± 18	4.7 ± 0.2	19.4 ± 1.7

[a] Values represent the mean (±range) of the data based on the accumulate errors in determining n_{PC} and m_{OG}. [b] The volume of the hydrophobic core of the micelles was calculated as the sum of the hydrophobic volumes of the amphiphile components using the estimates for the volume of the acyl chain region (Tanford, 1980): PC (1.62 nm^3) and OG (0.243 nm^3). [c] The surface area of the micelles was calculated as the sum of the surface areas of the amphiphile components using the estimates of 0.65 nm^2/PC and 0.38 nm^2/OG. [d] Surface area for an oblate or prolate ellipsoid having a minor axis of 1.16 nm and volume V (see Discussion and footnote 2).

Mixed Micelles Behave as a Phase. The observations in the present study support the notion that micelles can be considered a separate phase, an issue which is not well resolved [see, for example, Chapter 6 in Tanford (1980)]. There are several good arguments against using the term "phase" in connection with micelles, such as the lack of a sharp transition from monomers to micelles and the fact that the micellar phases cannot be separated from the rest of the aqueous solution. However, as outlined below, the results of Figure 3 and of Figure 5 indicate that mixed micelles demonstrate some characteristics of being a distinct phase.

The total concentration of OG needed to obtain mixed micelles of any given n_{PC} is shown in Figure 3 to depend linearly on [PC]. This linear dependence shows that the composition of these mixed micelles is not dependent on [PC], at least in the range studied ($0 < [PC] < 0.5$ mM), since, in that case, the lines should have curved. As shown above, the linearity of these dependencies can be explained by dividing the total amount of octyl glucoside in the cuvette into two categories: one free and one associated with lipid–detergent structures. If mixed micelles were aggregates of the amphiphile constituents, the composition of agregates should reflect the concentrations of both components. On the contrary, the data of Figure 3 indicate that, regardless of the total PC and OG concentrations, there is a defined correlation between the composition of PC–OG mixed micelles and the concentration of monomeric OG. Thus, mixed micelles behave as a distinct phase which is in equlibrium with the aqueous monomeric form of the detergent, and whose composition is determined by the usual requirement for equality of the activities of the detergent component in the two phases, aqueous and micellar.

The dependence of mixed micellar composition on the activity of monomeric OG (estimated by the intercepts of the lines in Figure 3) is also expected if mixed micelles behave as a phase (see Figure 5). There is a linear correlation between $[OG]_{aq}$ and the mole fraction of solute (i.e., PC) in the micelle. Specifically, the activity of monomeric octyl glucoside in equilibrium with mixed micelles depends linearly on the mole fraction of OG in micelles (χ_{OG}), as

$$[OG]_{aq} = \chi_{OG} cmc_0 \quad (6)$$

where cmc_0 is the cmc of pure OG. One simple explanation of this phenomenon, suggested by Tanford (1980), assumes that the micelles and the aqueous region are two separate phases in equilibrium and can be treated in a fashion similar to Raoult's law describing the activity of ideal gas dissolved in liquid. A different derivation of this relationship is given by Clint (1975).

Structure of Mixed Micelles. Although these experiments do not address the issue of micelle physical dimensions directly, the micelle compositions shown in Figure 4 put some constraints on the sizes and shapes of these mixed micelles. From the number of molecules per mixed micelle, it is clear that the micelle size becomes progressively smaller at higher octyl glucoside concentrations; i.e., at high n_{PC}, the micelles are quite large (total molecular weight 124 000) whereas at small n_{PC} the micelle weight is also small (27 000).

It is feasible to gain some insight about the shape of OG–PC mixed micelles from the composition data (Figure 4), if several assumptions are made regarding the structure of the micelles. If one requires that all polar head groups face the aqueous medium, that no hydrophobic surface is exposed to water, and that the acyl chain region is liquid hydrocarbon-like in nature, then the volume of the hydrophobic core and the surface area of the micelles are constrained to be equal to the sums of all amphiphile component acyl chain molecular volumes and head-group surface area, respectively (Table I). The acyl chain volume and extended length for these molecules can be estimated from the number of carbons in the chain [see Chapter 6 in Tanford (1980)]. For OG with an eight-carbon acyl chain, the volume and the extended length were calculated to be 0.243 nm^3 and 1.16 nm, respectively. Similarly, for PC, these values were estimated as 1.62 nm^3 and 2.2 nm (assuming 16 carbons per PC). We further assumed that the surface area per molecule in the micelle is similar to that determined in the lamellar phase [OG, 0.38 nm^2 (Ollivon et al., 1988); PC, 0.65 nm^2]. Thus, according to the data of Figure 4, the surface areas and hydrophobic core volumes of the mixed micelles could be estimated from the dimensions of the two amphiphile components.

Although many shapes may satisfy these constraints, it is possible to choose between two of the more popular models for micelle structures, the oblate vs prolate ellipsoid. Since the shorter amphiphile (OG) dominates the micelle composition, we chose to set the minor axis of the ellipsoid equal to the extended length of OG (1.16 nm). The major axis was calculated by equating the volume of the ellipsoid[2] to the volume of the micelle (Table I), and then the surface area of the ellipsoid was calculated.[2] Table I shows the comparison between the surface areas of the mixed micelles and those

[2] The volume (V) and surface area (S) of oblate ellipsoids are given by $V = 4\pi a^2 b/3$ and $S = 2\pi a^2 + (\pi b^2/\epsilon) \log [(1+\epsilon)/(1-\epsilon)]$ and for prolate ellipsoids by $V = 4\pi ab^2/3$ and $S = 2\pi b^2 + (2\pi ab/\epsilon) \sin^{-1} \epsilon$, where the major and minor axes are a and b, respectively, and $\epsilon = [1 - (b/a)^2]^{1/2}$ is the eccentricity.

predicted for prolate or oblate ellipsoids. The error in micelle composition determination was carried through all the calculations and is shown in Table I for the data of Figure 4 as well as for the ellipsoids. Although not identical, the surface areas calculated for the oblate ellipsoid are within the experimental error range, whereas the prolate values are larger than those for the mixed micelles and, for $n_{PC} > 10$, are beyond the error range. This suggests (but does not prove) that the micelles have an oblate disklike shape and are unlikely to be cigarlike.

The stoichiometry data shown in Figure 4 also suggest something about the micelle aggregation number of pure OG micelles. Extrapolated to $n_{PC} = 0$, the value for m_{OG} is about 38, i.e., 38 OG molecules in a pure OG micelle. Previous work has suggested that OG micelles have an aggregation number of between 27 (Jones et al., 1986) and 100 (Cabantchik & Darmon, 1984). If the OG micelle is spherical with a radius of 1.16 nm (the extended length of an OG acyl chain), then about 27 OG molecules could be accommodated per micelle according to our estimate of OG acyl volume (0.243 nm^3/OG). On the other hand, 44 OG head groups can be accommodated on the surface, if we assume that the surface area per molecule is 0.38 nm^2. Both numbers are clearly closer to the 38 molecules per micelle suggested by our data, than to 100.

On the other hand, an OG micelle can be nonspherical. If we then speculate that the micelle will be close to an oblate spheroid, following the mixed micelle observation, the dimensions can be calculated, assuming a minor axis of 1.16 nm, for micelle aggregation numbers of either 38 or 100 ($n = 27$ fits a sphere). For a micelle number of 38, the major axis would be 1.38 nm compared to 2.24 nm for 100 molecules per micelle. In both cases, the estimated surface areas agree within less than 22% with those calculated from the molecular surface areas. Thus, to distinguish between these two plausible compositions for a pure OG micelle, it is necessary to be able to discern the difference between an almost spherical structure (38 molecules) and one with one axis about twice the other (100 molecules).

Comparison with Other Phospholipid–Detergent Mixed Micelles. Knowledge of the characteristic features of lipid–detergent mixed micelles is of significant importance in choosing a detergent for a reconstitution procedure (Walter et al., 1988), and thus, a comparison between OG–PC mixed micelles and other systems might be useful. OG–egg PC micelles were found in this study to behave as an ideal phase in equilibrium with the aqueous OG. As $[OG]_{aq}$ increases, the mole fraction of PC decreases, and the micelles become smaller with both n_{PC} and m_{OG} decreasing. Egg PC–bile salt mixed micelles also have been shown to be in equilibrium with the aqueous detergent (Schurtenberger et al., 1985) since size, as determined by quasi-elastic light scattering, was a linear function of bile salt and PC concentrations. The bile salt–PC micelle size distribution indicates significant polydispersity (Mazer et al., 1980) and larger extended structures due to micelle aggregation as a function of ionic strength (Schurtenberger et al., 1985). In our analysis of PC–OG micelles, size and size distribution were not determined directly, but preliminary measurements using both quasi-elastic light scattering and gel chromatography suggest a monodisperse population. In contrast, for Triton–sphingomyelin micelles, within some concentration regimes, bimodal distributions were observed, using sedimentation velocity, column chromatography, and quasi-elastic light scattering (Yedgar et al., 1974; Robson & Dennis, 1978; Yedgar & Cooper, 1985). It should be noted that these investigators worked below the phase transition temperature for sphingomyelin which may have significantly constrained micelle shape. This is particularly plausible since monomodal distributions in size were observed at temperatures above the lipid phase transition temperature (Robson & Dennis, 1978), i.e., under conditions more analogous to the present experiments performed at 25 °C, well above the phase transition temperature for egg PC.

The Triton–sphingomyelin micelles (below the phase transition temperature for sphingomyelin) also differed from the OG–PC micelles in that the number of detergent molecules per micelle remained constant over a large range of phospholipid molecules (Yedgar et al., 1974; Yedgar & Cooper, 1985) whereas it is clear that for OG–egg PC micelles the number of OG molecules changes from about 84 molecules when $n_{PC} = 2$–3 to close to 350 molecules when $n_{PC} = 30$. Again, this difference is likely to be due to the transition temperature of the lipid.

Mixed micelles of GM1 gangliosides and the nonionic detergent $C_{12}E_8$ also have been examined by light scattering and analyzed (Corti et al., 1982) in terms of the model proposed by Clint (1974). In contrast to egg PC, GM1 itself forms micelles so that the GM1–$C_{12}E_8$ mixtures formed micelles in the entire range from 0 to 100 mol % GM1. In this case, Corti et al. (1982) observed that GM1 was replaced by $C_{12}E_8$ so that the total solid angle covered by the micelle components was constant, in contrast to OG–PC, where both components decreased simultaneously.

The oblate ellipsoid shape proposed for the Triton–sphingomyelin micelles also appears to be defined by the planar structure (or low radius of curvature) required by the lipid and the more highly curved structure adapted by Triton (Yedgar et al., 1974). Although anything we say about the OG–egg PC mixed micelles' shape is speculative, it is attractive to surmise that the more planar region of the oblate ellipsoid proposed above, on the basis of surface and volume constraints, is necessary to accommodate the egg PC whereas the OG occupies the more highly curved edge regions. Such a picture would also be consistent with that proposed for cholate–PC mixed micelles (Mazer et al., 1980; Small et al., 1969).

ACKNOWLEDGMENTS

We thank Dr. Michel Ollivon for his help throughout all stages of this work. We gratefully acknowledge helpful discussions and suggestions from Dr. James Cornette, Dr. David Siegel, and Dr. Stephen Morris and the help of Dr. Dean Astumian with the light-scattering measurements.

REFERENCES

Ames, B. N., & Durbin, D. T. (1960) *J. Biol. Chem. 235*, 769–775.

Cabantchik, Z. I., & Darmon, A. (1985) *CRC Crit. Rev. Biochem. 2*, 123–165.

Clint, J. H. (1975) *J. Chem. Soc. 71*, 1327–1334.

Corti, M., Deglorglo, V., Ghindoni, R., & Sonnino, S. (1982) *Biochemistry 86*, 2533–2537.

Dennis, E. A. (1986) *Adv. Colloid Interface Sci. 26*, 155–175.

Fromherz, P., & Ruppel, D. (1985) *FEBS Lett. 179*, 155–159.

Fung, B. K.-K., & Stryer, L. (1978) *Biochemistry 17*, 5241–5248.

Jackson, M. L., Schmidt, C. F., Lichtenberg, D., Litman, B. J., & Albert, A. D. (1982) *Biochemistry 21*, 4576–4582.

Jones, O. T., Earnest, J. P., & McNamee, M. G. (1986) in *Biological Membranes: A Practical Approach* (Findlay, J. B. C., Ed.) IRL, London.

Mazer, N. A., Benedek, G. B., & Carey, M. C. (1980) *Biochemistry 19*, 601-615.
Ollivon, M., Eidelman, O., Blumenthal, R., & Walter, A. (1988) *Biochemistry 27*, 1695-1703.
Robson, R. J., & Dennis, E. A. (1978) *Biochim. Biophys. Acta 508*, 513-524.
Schurtenberger, P., Mazer, N., & Kanzig, W. (1985) *J. Phys. Chem. 81*, 1042-1049.
Shinoda, K., Yamaguchi, T., & Hori, R. (1961) *Bull. Chem. Soc. Jpn. 34*, 237-241.
Small, D. M., Penkett, S. A., & Chapman, D. (1969) *Biochim. Biophys. Acta 176*, 178-189.
Struck, D. K., Hoekstra, D., & Pagano, R. E. (1981) *Biochemistry 20*, 4093-4099.
Tanford, C. (1980) *The Hydrophobic Effect: Formation of Micelles and Biological Membranes*, Wiley, New York.
Yedgar, S., & Cooper, V. G. (1985) *Arch. Biochem. Biophys. 240*, 191-200.
Yedgar, S., Barenholz, Y., & Cooper, V. G. (1974) *Biochim. Biophys. Acta 363*, 98-111.
Walter, A., Eidelman, O., Ollivon, M., & Blumenthal, R. (1988) in *Cellular Membrane Fusion: Fundamental Mechanisms and Applications of Membrane Fusion Techniques* (Wilschut, J., & Hoekstra, D., Eds.) Marcel Dekker, New York (in press).

Binding of Leukotriene C_4 to Rat Lung Fibroblasts and Stimulation of Collagen Synthesis in Vitro†

Sem H. Phan,* Bridget M. McGarry, Kathryn M. Loeffler, and Steven L. Kunkel
Department of Pathology, The University of Michigan Medical School, Ann Arbor, Michigan 48109
Received August 3, 1987; Revised Manuscript Received December 11, 1987

ABSTRACT: Arachidonate metabolites are potent biological mediators affecting multiple cellular functions. Although prostaglandins of the E series, which are products of the cyclooxygenase pathway, have been known as inhibitors or down-regulators of fibroblast proliferation and collagen synthesis, the more recently discovered products of the 5-lipoxygenase pathway have not been as extensively investigated with regard to fibroblast function. In this study, a sulfidopeptide product of the lipoxygenase pathway, leukotriene C_4 (LTC_4), was examined for its ability to modulate rat lung fibroblast collagen synthesis and proliferation in vitro. The data revealed the ability of LTC_4 and to a lesser extent leukotriene D_4 (LTD_4) to stimulate collagen synthesis in a dose-dependent (10^{-11}-10^{-8} M) manner without affecting cellular proliferation as determined by radiolabeled thymidine incorporation; 1 nM LTC_4 caused an 85% ($p < 0.02$) increase above untreated controls in [^{3}H]proline incorporation into collagenous protein in the media, which was blocked by the putative leukotriene receptor antagonist FPL55712 (10 μM) and inhibited by cycloheximide and actinomycin D. This LTC_4 stimulatory effect was slightly more specific for collagen synthesis vs noncollagenous protein synthesis but was not accompanied with any change in the collagen type composition. Binding of [^{3}H]LTC_4 to these cells was specific, reversible, and saturable, with a K_d of 1.8 ± 0.95 nM. Under equilibrium conditions, there was an estimated 2.39×10^4 receptors per cell. This binding was also inhibited by 10 μM FPL55712. Competitive binding studies show specificity of this binding for LTC_4 relative to LTD_4 and FPL55712. Furthermore, no significant conversion of LTC_4 to LTD_4 or leukotriene E_4 was noted during the binding studies. These results indicate the presence of specific LTC_4 receptors on these cells which may mediate the cellular effects on protein and collagen synthesis.

Understanding how arachidonate metabolites affect fibroblast growth and function is critical for uncovering the mechanism by which these substances initiate, maintain, and/or down-regulate the fibrogenic response in fibrotic diseases. Recent studies have demonstrated the inhibitory effects of prostaglandin E_2 (PGE_2)[1] on fibroblast growth and collagen synthesis (Baum et al., 1978; Clark et al., 1982; Elias et al., 1985), thus suggesting an important role as down-regulators, perhaps to maintain or return fibroblasts to a quiescent state. The more recently discovered 5-lipoxygenase pathway products of arachidonate metabolism have not been examined in as much detail. The products of this pathway are primarily the various HETE's and leukotrienes. These substances have diverse potent biological activities and are the products of various cell types (Samuelsson, 1983; Lewis & Austen, 1984).

† Supported by National Institutes of Health Grants HL28737, HL31237, HL31963, and HL39925 and by a grant-in-aid from the American Heart Association and its Michigan affiliate. Part of this work was performed during the tenure of Established Investigatorships (to S.H.P. and S.L.K.) of the American Heart Association.

* Address correspondence to this author at the Department of Pathology, Box 0602, The University of Michigan Medical School, 1301 Catherine St., Ann Arbor, MI 48109-0602.

[1] Abbreviations: PGE_2, prostaglandin E_2; LTB_4, leukotriene B_4; LTC_4, leukotriene C_4; LTD_4, leukotriene D_4; LTE_4, leukotriene E_4; DMEM, Dulbecco's modified Eagle's medium; βAPN, β-aminopropionitrile; PBS, phosphate-buffered saline; PMSF, phenylmethanesulfonyl fluoride; TCA, trichloroacetic acid; FCS, fetal calf serum; HETE, hydroxyeicosatetraenoic acid; 5-HETE, 5-hydroxyeicosatetraenoic acid; SRS-A, slow reactive substance of anaphylaxis; EDTA, ethylenediaminetetraacetic acid trisodium salt; PITC, phenyl isothiocyanate; PTH, phenylthiohydantoin; HPLC, high-performance liquid chromatography; SDS, sodium dodecyl sulfate; Tris-HCl, tris(hydroxymethyl)aminomethane hydrochloride.

0006-2960/88/0427-2846$01.50/0